

Hardware-Efficient EMG Decoding for Next-Generation Hand Prostheses

Mohammad Kalbasi^{1,2}, MohammadAli Shaeri¹, Vincent Alexandre Mendez³, Solaiman Shokur³,
Silvestro Micera³, Mahsa Shoaran¹

¹Institute of Electrical and Micro Engineering and Neuro-X Institute, EPFL, Geneva, Switzerland

²Department of Electrical Engineering, Sharif University of Technology, Tehran, Iran

³Bertarelli Foundation Chair in Translational Neuroengineering, Neuro-X Institute, EPFL, Geneva, Switzerland

Email: {mohammad.kalbasi, mohammad.shaeri, mahsa.shoaran}@epfl.ch

Abstract—Advancements in neural engineering have enabled the development of Robotic Prosthetic Hands (RPHs) aimed at restoring hand functionality. Current commercial RPHs offer limited control through basic on/off commands. Recent progresses in machine learning enable finger movement decoding with higher degrees of freedom, yet the high computational complexity of such models limits their application in portable devices. Future RPH designs must balance portability, low power consumption, and high decoding accuracy to be practical for individuals with disabilities. To this end, we introduce a novel attractor-based neural network to realize on-chip movement decoding for next-generation portable RPHs. The proposed architecture comprises an encoder, an attention layer, an attractor network, and a refinement regressor. We tested our model on four healthy subjects and achieved a decoding accuracy of $80.6 \pm 3.3\%$. Our proposed model is over 120 and 50 times more compact compared to state-of-the-art LSTM and CNN models, respectively, with comparable (or superior) decoding accuracy. Therefore, it exhibits minimal hardware complexity and can be effectively integrated as a System-on-Chip.

I. INTRODUCTION

Losing a hand is a devastating experience, profoundly affecting both a human’s physical and emotional well-being [1], [2]. Robotic Prosthetic Hands (RPHs) enhance amputees’ quality of life by restoring hand functionality. Such devices should mimic natural movements to induce sensations of the human hand [3], [4]. Hand prostheses first record Electromyographic (EMG) signals from a subject’s forearm, which consists of electrical activities generated by muscle contractions. In a classic example, the EMG signal recorded from two surface EMG electrodes (sEMG) was converted into a binary On/Off command for a robotic hand using a simple thresholding technique, enabling control with one degree of freedom [5]–[7]. Modern High-Density sEMG (HD-sEMG) electrodes are capable of recording from 128 channels and offer the potential to decode fine and dexterous movements from muscle activities [8]. Conventional EMG decoders have typically been developed for classifying different hand gestures [9]–[12]. In [13], a combined model incorporating kNN and Bayes classifiers was employed to decode four classes of hand gestures. Recently, a vision transformer model was utilized to classify as many as 65 hand gestures [14]. While such models achieve high accuracy in movement classification tasks, they lack the ability to decode a continuous movement trajectory, hindering the

naturalness of prosthetic hand movements.

To overcome this limitation, other studies have introduced AI solutions to continuously predict finger angles over time [15]–[19]. In [20], Independent Component Analysis (ICA) was used to isolate muscle activities associated with finger movements while a linear regressor predicted finger extension and flexion from forearm EMG. In another study, a Convolutional Neural Network (CNN) was utilized to simultaneously decode finger movements [21]. Given the proficiency of Recurrent Neural Networks (RNNs) in capturing intricate patterns, an encoder-decoder algorithm incorporating a Gated Recurrent Unit (GRU) with an attention mechanism was used to predict 14 finger joint angles [22]. Moreover, a Long Short-Term Memory (LSTM) model accompanying manifold learning and attention mechanism demonstrated promising results in decoding 22 joint angles [23].

In general, deep neural networks such as CNN and LSTM are recognized for their effectiveness in EMG decoding [21], [24], [25]. These methods are compute-intensive software solutions, requiring an external computer to process and decode EMG signals. The next generation of RPHs will offer seamless, portable prosthetic solutions that are user-friendly for individuals coping with hand loss, facilitating their daily activities. The evolution towards next-generation portable RPHs necessitates efficient integration with AI to directly translate EMG signals into movement commands, eliminating the need for an external computer. This approach follows the recent advancements in the intelligent neural interface domain with embedded AI [26]–[29]. Hence, model size and complexity must be prioritized in addition to decoding accuracy to ensure hardware efficiency [30]–[33]. To address these challenges, we propose a Dual Predictive Attractor-Refinement Strategy (DPARS) model for decoding continuous finger angles from EMG. Our proposed model achieves a significantly lower complexity by reducing the number of computations while maintaining accuracy comparable to state-of-the-art models such as CNN and LSTM.

II. MODEL ARCHITECTURE

The dual predictive algorithm is designed to simultaneously estimate coarse movements (using an attractor-based decoder) and fine motions (using an MLP regressor) to restore

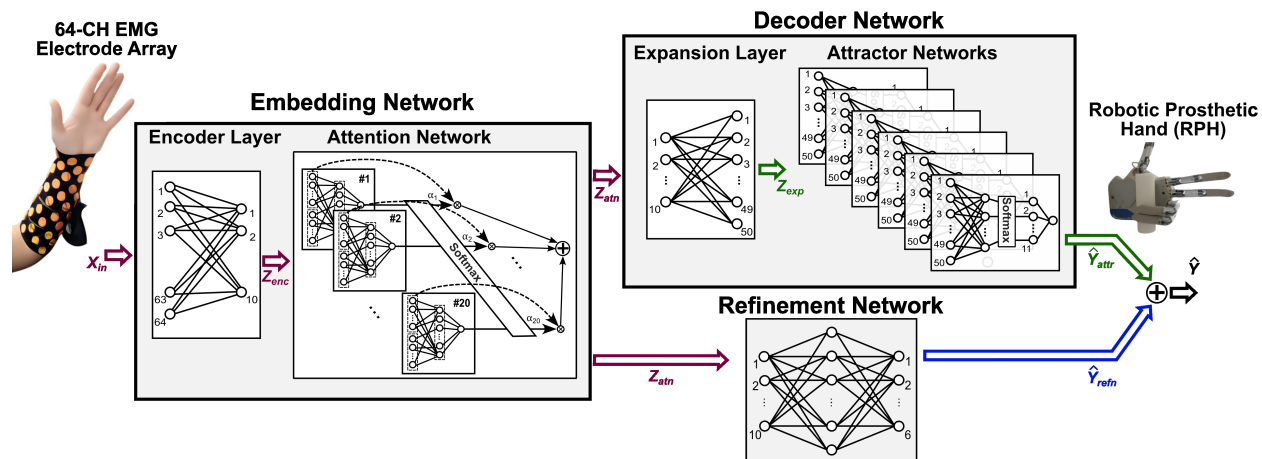


Fig. 1. Dual Predictive Attractor-Refinement Strategy (DPARS) for real-time EMG decoding. The model includes an encoder layer for dimensionality reduction, followed by an attention network that highlights the most important sample in a data stream. Then, the attractor network generates a coarse prediction (\hat{Y}_{attr}), while the refinement network refines the initial prediction by compensating for errors (\hat{Y}_{refn}). The decoded finger angle (\hat{Y}) will be generated by summing the coarse and the refinement signal.

natural, human-like control of RPHs. As depicted in Fig. 1, the proposed model predicts finger angles through the following steps: (i) An encoder network transforms the data representation from input space into a compact and informative embedding space. (ii) An attention network enables the model to focus on relevant information in the temporal sequence of data. (iii) A novel attractor network computes attractor state probabilities and generates a coarse estimation of the finger angles. (iv) A refinement network enhances the overall performance by assessing the initial prediction's errors. This two-level prediction mechanism, involving an attractor network and a refinement network, effectively ensures a robust and accurate prediction of finger angles.

A. Encoder Layer

Dimensionality reduction techniques, such as Independent Component Analysis (ICA) or Principal Component Analysis (PCA), have been demonstrated to be essential in EMG decoding [20], [34], [35]. Such techniques compress data by extracting informative features [36]. They can enhance prediction accuracy in addition to lowering the computational burden of following blocks in the decoding pipeline. Here, we designed a Single-Layer Perceptron (SLP) that functions as an encoder, efficiently mapping the EMG data into a compact representation. The SLP performs a linear transformation through matrix multiplication as follows:

$$Z_{enc}[i] = W_{enc} \times X_{in}[i] \quad (1)$$

where W_{enc} and $X_{in}[i]$ are the encoder weight matrix and the input at timestep i , respectively. Encoder weights are computed through an end-to-end training procedure using a global objective function (more details in Section II.C). Thanks to dimensionality reduction, the decoder solely processes low-dimensional encoded data. Thus, the number of computations is significantly reduced, resulting in a lower hardware cost.

B. Attention Network

The attention network learns patterns and assigns distinct weights to elements in a data sequence, emphasizing the most significant ones [37]. In this architecture, the attention mechanism is implemented using Multi-Layer Perceptrons (MLPs) with two layers that process a data stream comprising the current encoded data sample and the 19 preceding samples. The attention network consists of 20 sub-networks, each taking the two encoded data vectors at current time ($Z_{enc}[i]$) and j^{th} previous sample ($Z_{enc}[i-j]$) and calculating S_{atn} as:

$$S_{atn}[i, j] = W_{atn,2} \times \tanh \left(W_{atn,1} \begin{bmatrix} Z_{enc}[i-j] \\ Z_{enc}[i] \end{bmatrix} \right) \quad (2)$$

where W_{atn} indicates network weights and $S_{atn}[i-j]$ shows the attention scores for j^{th} previous sample in the sequence. Using a softmax function, normalized attention coefficients ($[\alpha[i, 0], \dots, \alpha[i, 19]] = \text{Softmax}(S_{atn}[i, 0], \dots, S_{atn}[i, 19])$) are extracted, representing the importance of each timestep. Then, a context vector as a weighted sum of attention coefficients and input sequence is determined:

$$Z_{atn}[i] = \sum_{j=0}^{19} \alpha[i, j] \times Z_{enc}[i-j]. \quad (3)$$

The context vector conveys a more condensed and information-rich representation of the encoded data sequence. It is worth mentioning that the attention network compresses the data stream in the time domain while the encoder reduces data dimensionally across input channels. The low-complexity MLP model implemented in this structure comprises a single hidden layer and an output layer. Moreover, the model is constrained to employ an identical network (i.e., with the same structure and weights) throughout training. Therefore, it can be implemented as a single MLP network and reused at different timesteps, resulting in a $20\times$ reduction in hardware cost compared to the conventional design.

C. Attractor Network

Fingers naturally exhibit a tendency to maintain specific positions between flexed and extended states despite their

free movement. This resembles attractors, a concept used in mathematics to describe the states that a dynamical system tends to end up in [38], [39]. Inspired by this concept, we introduce a novel attractor-based network that extracts the most probable states (attractors) and predicts the output based on their probability distributions. To address complexity and accuracy concerns, we limit the search domain for attractor extraction to eleven discrete states, encompassing a range from fully flexed (90°) to fully extended (180°). Figure 1 illustrates the attractor networks within a decoder network positioned after an expansion layer. The expansion layer enhances the model’s capability to extract more intricate patterns by mapping the context vector to a higher-level feature space. Then, the attractor network utilizes two-layer MLPs to assess the likelihood of each individual state in the attractor set (\mathcal{K}) for each finger. It generates an initial estimate of a finger angle by computing a sum of attractor values weighted by their associated likelihoods, expressed as:

$$\hat{Y}_{\text{attr}}^c = \sum_{k \in \mathcal{K}} k \times Pr(Y_q^c = k) \quad (4)$$

where Y_q^c is a random variable representing the likelihood of each discrete attractor state for the corresponding finger c . The probability distribution of Y_q^c is generated by the attractor network, quantifying the likelihoods for each state and determining the probabilistic prediction of finger angles.

The attractor-based decoder is trained along with the embedding network to predict outputs by leveraging the most probable states. The model is trained using an objective function aimed at minimizing the l_1 loss and identifying the attractors. The objective function is defined as:

$$G(\theta) = \mathbb{E}_{X,Y} \left[\|\hat{Y}(X; \theta) - Y\|_1 + \lambda \sum_{c=1}^6 H(Y_q^c(X; \theta)) \right] \quad (5)$$

where Y and \hat{Y} are the real and predicted finger angles, respectively. θ denotes the parameter set of the model and H is the entropy operator. The entropy term has a key role in extracting attractors by assigning only a few highly probable states to the attractor set.

D. refinement Network

The decoder network provides a coarse yet accurate initial estimation based on attractors. In parallel, a refinement network is incorporated into the model to improve the naturalness of RPH movements by capturing fine details. In this design, a two-layer MLP regressor is used to predict complementary movements for each finger angle. By adding this signal to the initial prediction, the DPARS output is determined as follows:

$$\hat{Y} = \hat{Y}_{\text{attr}} + \hat{Y}_{\text{refn}} \quad (6)$$

where Y_{attr} and Y_{refn} denote the output of the attractor network and refinement network, respectively. By summing these two signals, the proposed model effectively decodes the coarse and fine activities in intricate movements. This dual predictive strategy enhances the prediction accuracy, robustness, and naturalness of the movement decoding.

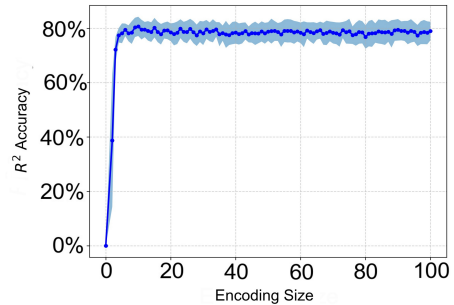


Fig. 2. Impact of Encoding Size on Decoding Accuracy: The blue line represents the mean R^2 accuracy against the encoding size, and the shaded area indicates the variance.

III. RESULTS

In this study, we recorded EMG and finger movements from four healthy subjects, ethically approved by the Cantonal Ethical Committee of Vaud, while all participants provided informed consent for participating in the study. Each subject was tasked with replicating various finger movements and grasps, as demonstrated in the pre-captured videos provided by our research team. These movements involved flexing, extending, or maintaining a middle position (rest) of the fingers. The video sequences were repeated six times. Participants were instructed to mimic the finger movements displayed in the videos. The first four repetitions were dedicated to the training dataset. The fifth and sixth repetitions were separately allocated to the validation and test datasets, ensuring robust evaluation of the model’s predictive performance.

The EMG data was acquired using a Medium Density EMG (MD-EMG) system with 64 monopolar channels and dry electrodes [40]. The signals were captured at a frequency of 2400 Hz and filtered with a bandpass filter within a range of 5 to 500 Hz, along with a 50 Hz notch filter to remove the power line interference. Next, the envelope of the EMG signal was extracted by applying a low-pass filter to the absolute value of the signal and then downsampled at a rate of 100 Hz ($T_s=10\text{ms}$). The input data stream is then segmented into 200 ms data blocks with 190 ms overlap between windows, which is equal to 20 data samples per block for predicting each output. The proposed DPARS algorithm is implemented using the PyTorch toolkit in Python. All blocks in DPARS are designed based on feedforward fully connected MLP architecture to optimize computational efficiency and minimize model complexity. The model parameters are learned by minimizing the entropy-regularized loss function described in Eq. (5) using the Stochastic Gradient Descent (SGD) optimizer with a batch size of 64 for 100 epochs. During model training, the parameters yielding the lowest validation loss are ultimately used as the final configuration of the model. The performance is assessed with the normalized error measured by the R^2 metric on the test sets between predicted and real finger angles.

A. Computational Efficiency of the Model

The encoder network transforms the 64-ch EMG data into a more compact and informative representation. Figure 2 illustrates the prediction accuracy against the encoding size.

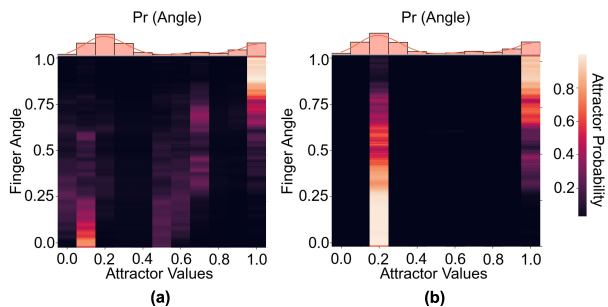


Fig. 3. Probability distributions generated by the attractor network. (a) Probability distribution spread among all possible states through minimizing decoder loss only. (b) The network extracts attractors. The probability of non-attractor states equals zero when the entropy regularization term is included in the objective function, leading to $>4\times$ less number of computations.

DPARS achieves its optimal performance with an encoding size of ten, resulting in a significant reduction of $6.4\times$ in dimensionality. Then, the attention network processes encoded data for 20 consecutive timesteps (i.e., with 20×10 dimensions) and generates a context vector (i.e., with a dimension of 10), yielding an additional $20\times$ dimensionality reduction. Thanks to reducing encoding size and data dimensionality, the number of Multiply–Accumulate (MAC) operations and the required memory are decreased by a factor of 128 (6.4×20) in the subsequent layers.

The attractor network induces sparsity in data representation by penalizing high entropy values. As a result, the probabilities are only assigned to a specific attractor, and the output is a weighted sum of the attractor states. This has the potential to reduce the hardware cost and the number of MAC operations by $>4\times$. Figure 3(a) illustrates the state probabilities estimated without entropy regularization. Incorporating the entropy term into the objective function (eq. (5)), the data distribution is notably concentrated on two distinct states (attractors) as shown in Fig. 3(b). The attractor network essentially captures attractors and generates a relatively coarse prediction. It allows the refinement network to focus on fine details and refine the coarse prediction. This dual predictive strategy incorporating entropy regularization boosts decoding accuracy by more than 3%, as shown in Table I.

B. Performance Evaluation and Comparison

In this section, we evaluate the complexity and accuracy of the proposed DPARS model and compare it with other state-of-the-art EMG decoders. The R^2 score and total number of parameters are used to measure the decoding accuracy and to estimate the model size, respectively. Table I compares

TABLE I
PERFORMANCE COMPARISON OF THE PROPOSED MODEL AND
STATE-OF-THE-ART MODELS

Model Name	R^2 Score					No. Parameters
	Subject 1	Subject 2	Subject 3	Subject 4	Average of All Subjects	
SVR (RBF)	0.749	0.359	0.421	0.615	0.536	N/A
CNN	0.814	0.725	0.797	0.682	0.755	337670
LSTM (1 Layer)	0.867	0.780	0.824	0.712	0.796	519212
LSTM (2 Layer)	0.876	0.782	0.827	0.737	0.806	840812
LSTM (3 Layer)	0.884	0.781	0.836	0.758	0.815	1162412
DPARS	0.834	0.748	0.787	0.745	0.778	6828
DPARS (+entropy)	0.853	0.773	0.821	0.778	0.806	6828

* Since the kernelized SVR is a non-parametric model, the number of parameters depends on the size of the training data [41].

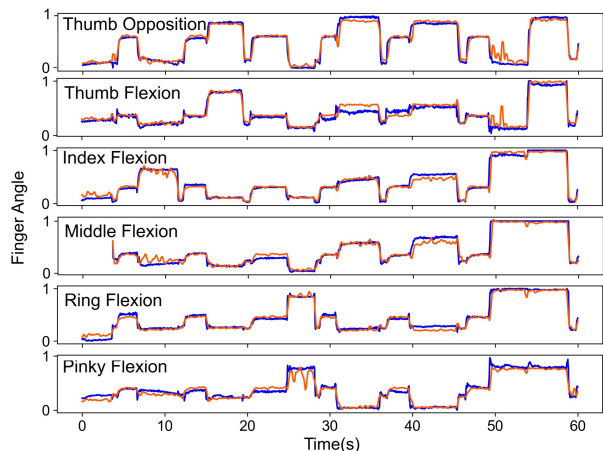


Fig. 4. The real (blue line) and decoded (orange line) figure angles predicted by the proposed DPARS model.

the performance of LSTM [23], deep CNN [21], and support vector regression (SVR) [19] with the proposed DPARS.

We found that SVR exhibits a low accuracy of 53.6% on average, even with an RBF kernel. CNN demonstrated a mean decoding accuracy of 75.5%, while LSTM outperforms CNN and SVR with an accuracy of $<81.5\%$. These models are characterized by their large sizes, featuring several hundred thousand parameters. Consequently, implementing such models in hardware would lead to large silicon area and high power consumption, making them impractical for next-generation lightweight RPHs. Our novel attractor-based model decodes EMG signal with a mean accuracy of 80.6% using a total of 6828 parameters. Figure 4 illustrates the ground truth finger angles and the predicted output of the proposed decoder. This figure displays the decoder’s proficiency in estimating finger movement angles across all angles, with the highest accuracy observed in the thumb opposition and ring flexion. These promising results show that DPARS achieves a comparable or superior performance in EMG decoding compared to LSTM and CNN, respectively. Furthermore, our proposed model, while $>50\times$ smaller than existing models, maintains competitive decoding performance and offers significant advantages in terms of reduced model complexity and energy efficiency.

IV. CONCLUSION

This study proposed an innovative DPARS model for EMG decoding, employing a dual predictive strategy. The model initially provides a coarse estimation based on attractors, capturing the underlying patterns in EMG signals, and then refines this estimation using a lightweight regressor. Owing to the extensive dimensionality reduction, weight sharing, and dual predictive strategy, DPARS exhibits a remarkable reduction in model size, more compact than LSTM and CNN models by a factor of 50 to 120, respectively. Furthermore, the decoder network only needs to compute the attractors’ likelihood (i.e., not for all states), resulting in more than a fourfold reduction in the number of MAC operations. We proved DPARS is accurate, compact, and low-complexity, making it well-suited for lightweight and accessible AI-enabled hand prostheses that can significantly improve the quality of life of amputees.

REFERENCES

- [1] C. L. McDonald, S. Westcott-McCoy, M. R. Weaver, J. Haagsma, and D. Kartin, "Global prevalence of traumatic non-fatal limb amputation," *Prosthetics and Orthotics International*, vol. 45, no. 2, pp. 115-125, Apr. 2020.
- [2] M. Grob, N. A. Papadopulos, A. Zimmermann, E. Biemer, and L. Kovacs, "The Psychological Impact of Severe Hand Injury," *Journal of Hand Surgery (European Volume)*, vol. 33, no. 3, pp. 358-362, Jun. 2008.
- [3] G. S. Dhillon and K. W. Horch, "Direct neural sensory feedback and control of a prosthetic arm," *IEEE Transactions on Neural Systems and Rehabilitation Engineering*, vol. 13, no. 4, pp. 468-472, Dec. 2005.
- [4] G. N. Saridis and T. P. Gootee, "EMG Pattern Analysis and Classification for a Prosthetic Arm," *IEEE Transactions on Biomedical Engineering*, vol. BME-29, no. 6, pp. 403-412, Jun. 1982.
- [5] P. Geethanjali, "Myoelectric control of prosthetic hands: State-of-the-art review," *Medical Devices: Evidence and Research*, vol. 9, pp. 247-255, Jul. 2016.
- [6] C. Gentile, F. Cordella, and L. Zollo, "Hierarchical human-inspired control strategies for prosthetic hands," *Sensors*, vol. 22, no. 7, pp. 2521, Mar. 2022.
- [7] V. Mendez, F. Iberite, S. Shokur, and S. Micera, "Current solutions and future trends for robotic prosthetic hands," *Annual Review of Control, Robotics, and Autonomous Systems*, vol. 4, pp. 595-627, May 2021.
- [8] N. Malešević, A. Olsson, P. Sager, E. Andersson, C. Cipriani, M. Controzzi, A. Björkman, and C. Antfolk, "A database of high-density surface electromyogram signals comprising 65 isometric hand gestures," *Scientific Data*, vol. 8, no. 63, pp. 1-10, Feb. 2021.
- [9] K. Englehart and B. Hudgins, "A Robust, Real-Time Control Scheme for Multifunction Myoelectric Control," *IEEE Transactions on Biomedical Engineering*, vol. 50, no. 7, pp. 848-854, Jun. 2003.
- [10] M. Atzori et al., "Characterization of a benchmark database for myoelectric movement classification," *IEEE Transactions on Neural Systems and Rehabilitation Engineering*, vol. 23, no. 1, pp. 73-83, Jan. 2015.
- [11] S. Zabihi, E. Rahimian, A. Asif, and A. Mohammadi, "TraHGR: Transformer for Hand Gesture Recognition via Electromyography," *IEEE Transactions on Neural Systems and Rehabilitation Engineering*, vol. 31, pp. 4211-4224, Oct. 2023.
- [12] D. Esposito et al., "A piezoresistive array armband with reduced number of sensors for hand gesture recognition," *Frontiers in Neurobotics*, vol. 13, p. 114, Jan. 2020.
- [13] J. Kim, S. Mastnik, and E. André, "EMG-based hand gesture recognition for real-time biosignal interfacing," in *Proceedings of the 13th International Conference on Intelligent User Interfaces*, 2008, pp. 30-39.
- [14] M. Montazerin, E. Rahimian, F. Naderkhani, S. Atashzar, S. Yanshkevich and A. Mohammadi, "Transformer-based hand gesture recognition from instantaneous to fused neural decomposition of high-density EMG signals," *Scientific Reports*, vol. 13, Jul. 2023, Art. no.11000.
- [15] P. Afshar and Y. Matsuoka, "Neural-based control of a robotic hand: evidence for distinct muscle strategies," in *IEEE International Conference on Robotics and Automation*, Vol. 5, 2004, pp. 4633-4638.
- [16] M. Hioki and H. Kawasaki, "Estimation of Finger Joint Angles from sEMG Using a Neural Network Including Time Delay Factor and Recurrent Structure," *International Scholarly Research Notices*, vol. 2012, pp. 1-13, 2012.
- [17] R. J. Smith, F. Tenore, D. Huberdeau, R. Etienne-Cummings, and N. V. Thakor, "Continuous decoding of finger position from surface EMG signals for the control of powered prostheses," in *IEEE Engineering in Medicine and Biology Society Conference*, 2008, pp. 197-200.
- [18] J. G. Ngeo, T. Tamei, and T. Shibata, "Continuous and simultaneous estimation of finger kinematics using inputs from an EMG-to-muscle activation model," *Journal of Neuroengineering and Rehabilitation*, vol. 11, no. 1, pp. 1-14, Dec. 2014.
- [19] L. Pan, D. Zhang, J. Liu, X. Sheng, and X. Zhu, "Continuous estimation of finger joint angles under different static wrist motions from surface EMG signals," *Biomedical Signal Processing and Control*, vol. 14, pp. 265-271, Nov. 2014.
- [20] S. Stapornchaisit, Y. Kim, A. Takagi, N. Yoshimura, and Y. Koike, "Finger angle estimation from array EMG system using linear regression model with independent component analysis," *Frontiers in Neurobotics*, vol. 13, Sep. 2019, Art. no. 75.
- [21] V. Mendez, L. Pollina, F. Artoni, and S. Micera, "Deep learning with convolutional neural network for proportional control of finger movements from surface EMG recordings," in *IEEE/EMBS Conference on Neural Engineering*, 2021, pp. 1074-1078.
- [22] H. Lee, D. Kim and Y. L. Park, "Explainable Deep Learning Model for EMG-Based Finger Angle Estimation Using Attention," *IEEE Transactions on Neural Systems and Rehabilitation Engineering*, vol. 30, pp. 1877-1886, Jul. 2022.
- [23] C. Avian, S. W. Prakosa, M. Faisal, and J.-S. Leu, "Estimating finger joint angles on surface EMG using manifold learning and long short-term memory with attention mechanism," *Biomedical Signal Processing and Control*, vol. 71, 2022, Art. no. 103099.
- [24] A. Ameri, M. A. Akhaee, E. Scheme, and K. Englehart, "Regression convolutional neural network for improved simultaneous EMG control," *Journal of Neural Engineering*, vol. 16, no. 3, 2019, Art. no. 036015.
- [25] R. B. Azhiri, M. Esmaeili, and M. Nourani, "Real-time EMG signal classification via recurrent neural networks," in *IEEE International Conference on Bioinformatics and Biomedicine*, Dec. 2021, pp. 2628-2635.
- [26] M. Shoaran, B. A. Haghi, M. Taghavi, M. Farivar, A. Emami, "Energy-Efficient Classification for Resource-Constrained Biomedical Applications," in *IEEE Journal on Emerging and Selected Topics in Circuits and Systems (JETCAS)*, pp. 693-707, 2018.
- [27] M. Shoaran, "Next-Generation Closed-Loop Neural Interfaces: Circuit and AI-driven innovations," in *IEEE Solid-State Circuits Magazine*, pp. 41-49, 2023.
- [28] B. Zhu, U. Shin, M. Shoaran, "Closed-loop neural prostheses with on-chip intelligence: A review and a low-latency machine learning model for brain state detection," in *IEEE transactions on biomedical circuits and systems*, pp. 877-897, 2021.
- [29] U. Shin et al., "A 256-channel 0.227- μ J/class versatile neural activity classification and closed-loop neuromodulation SoC," *IEEE Journal of Solid-State Circuits*, pp. 3243-3257, 2022.
- [30] M. A. Shaeri, A. Afzal, and M. Shoaran, "Challenges and Opportunities of Edge AI for Next-Generation Implantable BMIs," in *IEEE International Conference On Artificial Intelligence Circuits And Systems*, 2022, pp. 190-193.
- [31] J. Yoo, M. Shoaran, "Neural interface systems with on-device computing: Machine learning and neuromorphic architectures," in *Current opinion in biotechnology*, pp. 95-101, 2021.
- [32] M. Shoaran, U. Shin, M. A. Shaeri, "Intelligent Neural Interfaces: An Emerging Era in Neurotechnology," in *IEEE Custom Integrated Circuits Conference (CICC)*, pp. 1-7, 2024.
- [33] B. Zhu, M. Farivar, M. Shoaran, "ResOT: Resource-Efficient Oblique Trees for Neural Signal Classification," in *IEEE Transactions on Biomedical Circuits and Systems*, pp. 692-704, 2020.
- [34] L. Dela, D. Sutopo, S. Kurniawan, T. Tjahjowidodo, and W. Caesarendra, "EMG Based Classification of Hand Gesture Using PCA and SVM," in *International Conference on Electronics, Biomedical Engineering, and Health Informatics*, Nov. 2022, pp. 459-477.
- [35] W. Caesarendra, T. Tjahjowidodo, and D. Pamungkas, "EMG based classification of hand gestures using PCA and ANFIS," in *International Conference on Robotics, Biomimetics, and Intelligent Computational Systems*, 2017, pp. 18-23.
- [36] M. A. Shaeri and A. M. Sodagar, "Data Transformation in the Processing of Neuronal Signals: A Powerful Tool to Illuminate Informative Contents," *IEEE Reviews in Biomedical Engineering*, vol. 16, pp. 611-626, Feb. 2022.
- [37] Z. Niu, G. Zhong, and H. Yu, "A review on the attention mechanism of deep learning," *Neurocomputing*, vol. 452, pp. 48-62, Sep. 2021.
- [38] J. Milnor, "On the Concept of Attractor," *Communications in Mathematical Physics*, vol. 99, pp. 177-195, Jun. 1985.
- [39] A. Finkelstein, L. Fontolan, M. N. Economio, et al., "Attractor dynamics gate cortical information flow during decision-making," *Nature Neuroscience*, vol. 24, no. 6, pp. 843-850, Jun. 2021.
- [40] V. A. Mendez, "Improving hand prosthesis control with advanced single-finger proportional decoding and robotic shared control," Ph.D. dissertation, EPFL, 2023.
- [41] S. J. Russell and P. Norvig, *Artificial Intelligence: A Modern Approach*, Third edition, Pearson, 2010.